SUPPLEMENTAL MATERIALS

TEXT S1

The original duckweed family Lemnaceae (Hegelmaier 1895) was shown to be monophyletic with the family Araceae (Cabrera *et al.* 2008; Cusimano *et al.* 2011; Nauheimer, Metzler & Renner 2012). Although the Angiosperm Phylogeny III suggested therefore to include duckweeds as a subfamily of Araceae (Lemnoideae), most duckweed researcher consider them as a separate family, Lemnaceae (Appenroth, Borisjuk & Lam 2013; Appenroth & Crawford 2015; Sree, Bog & Appenroth 2016).

TEXT S2

Material and Methods

Establishment of a database of fluorescence emission spectra for major *S. polyrhiza* flavonoids - details

To test for the linearity of the fluorescence and to compare the fluorescence intensities among the individual compounds, standard curves of fluorescence intensities of each individual synthetic flavonoid were recorded on cLSM as described in the main manuscript for final concentrations between 0 and 2.5 mM in DMSO after 1:1 addition of 0.25 % 2-APB solution. To investigate the effect of pH on the emission spectra, we further recorded the spectra of individual 2-APB conjugated compounds under varying pH conditions using potassium phosphate buffer with a pH of 5.7, 7.3 and 8. To test for the effect of DMSO and 2-APB concentration on the flavonoid emission spectra, we additionally recorded the spectra of compounds dissolved in a lower DMSO concentration (25 vs 5 % of solution drop) as well as a lower 2-APB concentration (0.25 % vs 0.13 % of stock solution). As the absolute intensity of a 2-APB stained flavonoid glucoside of a given concentration in a drop of standard solution largely depended on the focus plane, we standardized the measurements by choosing the focus at the maximal

intensity within a defined area of each image (fourth quadrant of each image) for all *in vitro* studies. For *in vivo* recordings chloroplasts were chosen as the focus plane as these were easily detectable in the chlorophyll channel and therefore independent of investigating flavonoids within the plant body. Due to technical limitations the extraction of spectra of a homogenous flavonoid glucoside mixed standard solution is not possible: The laser excites more than one molecule (fluorophore of flavonoid glucoside/2-APB) at a time resulting in a "mixed" signal. However, once the spectrum of each individual compound solution is extracted and stored in the database, channels can be assigned in parallel pixel by pixel *in vivo*. Our chosen cLSM settings of 21 % transmission, 625 gain, pinhole 39 µm were chosen based on preliminary investigations observing the range of *in vivo* fluorescence intensities of images under highest (copper treatment) and lowest (AIP -- PAL-inhibitor) treatment.

TEXT S3

Material and Methods

Visualization and quantification of secondary fluorescence across tissue layers of the *S. polyrhiza* frond - statistics

To test whether individual compounds are distributed differentially across tissue layers, we used linear mixed model analysis with tissue layer as fixed effect and the individual frond as random effect. *P*-values were obtained by likelihood ratio tests that compare the full model with the reduced model in which tissue layer was removed as a fixed effect. Pairwise comparisons were obtained with Tukey's posthoc test.

TEXT S4

Material and Methods

Verification of cLSM-based flavonoid visualization *in vivo* – details

Three fronds of very similar appearance (each a single mature mother frond with one emerging daughter frond attached to it) were placed into 250 mL plastic bowls filled with 180 mL full nutrient medium without and with 2 µM AIP (n=12). After four days, a single mature plant of the second generation (granddaughters) of half of the replicates of each treatment was used for cLSM analysis utilizing the 'online fingerprinting' feature as described above. The granddaughter generation was used as these plants fully developed under the specific conditions and as the plants displayed stable flavonoid levels at this age (see below). The granddaughter fronds of the remaining replicates of each treatment were briefly dried, weighed and immediately frozen in liquid nitrogen to determine flavonoid concentration using high pressure liquid chromatography (HPLC). Plant material for HPLC analysis was stored at -20 °C until extraction. For flavonoid extraction, frozen plant tissue was ground by vigorously shaking the tubes with three metal beads for 1 min in a paint shaker. Fifty mg powdered tissue was then extracted with 1 ml 100% methanol (or adjusted volume if less than 50 mg was available) by vortexing for 8 s. Samples were centrifuged for 10 min at room temperature at 17,000 g. The supernatant was stored at -20 °C prior to HPLC analysis.

Methanol extracts were analysed by HPLC 1100 series equipment (Agilent Technologies) coupled to a photodiode array detector (G1315A DAD, Agilent Technologies). Analyte separation was accomplished with a Nucleodur Sphinx RP column (250 4.6 mm, 5 µm particle size, Macherey-Nagel). Injection volume was 10 µl. The mobile phase consisted of 0.2 % formic acid in water (solvent A) and acetonitrile (solvent B) at a flow rate of 1 ml min^{-1} using the following gradient: 0 min 10 % (B), 8 min 21 % (B), 17.0 min 55 % (B), 17.1 min 100 % (B), 18.0 min 100 % (B), 18.1 min 10 % (B), 22 min 10 % (B). Peak areas of the four major flavonoids, lut 8-C-glc, lut 7-O-glc, ap 8-C-glc and ap 7-O-glc, were integrated at 330 nm and quantified based on external standards of lut 7-O-glc and adjusted for the

molecular weight of the individual flavonoids (factors for luteolins and apigenins were 1 and 0.96, respectively).

To test the effect of AIP on flavonoid concentrations, we compared mean flavonoid levels between control and AIP treated plants using Student's *t*-test. Fluorescence intensities were extracted with ImageJ as described above. To test whether individual compounds were distributed differentially across tissue layers of fronds grown in the presence of AIP, we used linear mixed model analysis with tissue layer as fixed effect and the individual frond as random effect. *P*-values were obtained by likelihood ratio tests that compare the full model with the reduced model in which tissue layer was removed as fixed effect. Pairwise comparisons were obtained with Tukey's posthoc test. To test whether AIP had tissue layer effects on flavonoid reduction, we used linear mixed model analysis with tissue layer, treatment and their interaction as fixed effects and individual frond as random effect for each metabolite separately. *P*-values were obtained by likelihood ratio tests that compare the full model with the model in which the interaction of tissue layer and treatment was removed (tissue layer specific effects of AIP). Wilcoxon Mann Whitney Test were then used to test for differences in individual flavonoid glucoside fluorescence intensities between treatments within each tissue layer.

TEXT S5

Material and Methods

Tissue-specific induction of flavonoids under copper sulphate treatment – statistics

To test the effect of copper sulphate addition on biomass production, we compared mean biomass of fronds grown in the absence and presence of copper sulphate addition using Student's *t*-test. To test the effect of copper sulphate addition on flavonoid concentrations, we compared mean flavonoid levels between control and copper-induced plants using Student's *t*-test. To test for differences in the magnitude of induction across the four major flavonoids, we divided the metabolite concentration of each copper-treated plant by the mean of the control plants for each flavonoid individually (relative induction). Differences in the relative induction across the four flavonoids were analysed using one-way

ANOVA. Pairwise comparisons were performed with Tukey's posthoc test. To test whether copper exposure had tissue layer specific effects on flavonoid induction, we used linear mixed model analysis of fluorescence intensity data with tissue layer, treatment and their interaction as fixed effects and individual frond as random effects for each metabolite separately. *P*-values were obtained by likelihood ratio tests that compare the full model with the model in which the interaction of tissue layer and treatment was removed (tissue layer specific effects of copper treatment). Wilcoxon-Mann-Whitney-Tests were then used to test for differences in fluorescence intensities between treatments within each tissue layer.

TEXT S6

Material and Methods

Induction of flavonoids under natural UV light – statistics

To test the effect of UV radiation on biomass production, we compared biomass between fronds grown in the absence and presence of UV light using Student's *t*-test. To test the effect of UV radiation on flavonoid concentrations, we compared mean flavonoid levels between control and UV treated plants using Student's *t*-test. To test for differences in the magnitude of induction across the four major flavonoids, we divided the metabolite concentrations of the UV-treated plants by the mean of the control plants for each flavonoid individually (relative change). Differences in the relative change across the four flavonoids were analysed using one-way ANOVA. Pairwise comparisons were performed with Tukey's posthoc test. To test whether UV radiation had tissue layer-specific effects on flavonoid induction, we used linear mixed model analysis of fluorescence intensity data with tissue layer, treatment and their interaction as fixed effects and individual frond as random effects for each metabolite separately. *P*-values were obtained by likelihood ratio tests that compared the full model with the model in which the interaction of tissue layer and treatment was removed (tissue layer specific effects of UV

stress). Wilcoxon-Mann-Whitney-Tests were then used to test for differences in fluorescence intensities between treatments within each tissue layer.

TEXT S7

Material and Methods

Fitness assay of genotypes exposed to copper sulphate -statistics:

Differences in biomass production between copper sulphate-treated and control plants were analysed with a paired Student's *t*-test using the mean value of each genotype and treatment. Biomass production is an excellent predictor for plant fitness in this almost exclusively vegetative reproducing plant and incorporates both the effect of resistance (reduced damage) and tolerance (growth despite damage). The correlations among the individual flavonoid concentrations were analysed using Pearson's moment correlations using the mean values of each clone under control conditions. *P*-values of Pearson's correlation coefficients were obtained using the Hmisc package (Harrell Jr & Dupont 2015). To assess the correlation between plant fitness and flavonoid concentrations, we normalized growth variation among genotypes by expressing the mean biomass accumulation of copper-exposed plants relative to the mean biomass production under control conditions of each genotype ("relative fitness"). The correlations between relative fitness and constitutive as well as induced flavonoid levels were analysed with linear models for each metabolite individually as well as for total flavonoid concentration (sum of the four major flavonoids). To assess the relation between absolute growth and flavonoid concentrations, the correlations between total fresh mass and individual as well as total flavonoid concentration in the presence and absence of $CuSO_4$ were analysed using linear models based on the mean value of each treatment and genotype.

TEXT S8

Material and Methods

Fitness assay of genotypes exposed to ambient UV light – statistics:

Difference in biomass production between UV-shielded and -exposed conditions was analysed by a paired Student's *t*-test using the mean value of each genotype and treatment. Analogous to the correlations of plant fitness and flavonoid concentrations under copper stress, we standardized the growth between genotypes by expressing the mean biomass accumulation under UV-exposed conditions relative to the mean biomass production under UV-shielded conditions of each genotype ("relative fitness"). Correlations between relative fitness and constitutive as well as induced flavonoid levels were analysed with linear models for each metabolite separately as well as for total flavonoid concentration. To assess the relation between absolute growth and flavonoid concentrations, the correlations between total fresh mass and individual as well as total flavonoid concentrations under UV-exposed and -shielded conditions were analysed using linear models based on the mean value of each treatment and genotype. The correlation between relative fitness under UV light and under copper sulphate exposure was analysed with a linear model.

164 **TABLE S1** *Spirodela polyrhiza* accessions used for fitness experiments (1 = used; 0 = not used).

Accession Number	UV experiment	copper experiment	Continent	Country
8756	1	1	Africa	Ethiopia
8683	1	1	Africa	Kenya
9510	1	1	Africa	Mozambique
9907	1	1	Asia	Bangladesh
9925	1	0	Asia	Bangladesh
0040	1	1	Asia	China
9636	1	1	Asia	China
5523	1	0	Asia	China
0109	1	0	Asia	China
0092	1	1	Asia	China
5521	1	1	Asia	China
0090	0	1	Asia	China
0225	0	1	Asia	China
9668	0	1	Asia	China
9503	1	1	Asia	India
7379	1	1	Asia	India
8442	1	1	Asia	India
9650	1	1	Asia	India
9295	1	1	Asia	India
9305	0	1	Asia	India
9290	0	1	Asia	India
8787	0	1	Asia	Nepal
7674	1	1	Asia	Nepal
9507	1	1	Asia	Russia
9511	1	1	Asia	Russia
9512	0	1	Asia	Russia
9351	1	1	Asia	Vietnam
0013	0	1	Asia	Vietnam
7551	1	1	Australia	Australia
9625	1	1	Europe	Albania
9628	1	1	Europe	Albania
9633	1	0	Europe	Albania
9629	1	0	Europe	Albania
9514	1	1	Europe	Austria
9513	0	1	Europe	Czech Republic
9256	0	1	Europe	Finland
8403	0	1	Europe	France
9509	1	1	Europe	Germany
9500	1	1	Europe	Germany
5513	0	1	Europe	Germany
5501	0	1	Europe	Hungary
9502	1	1	Europe	Ireland
9618	1	1	Europe	Italy
9413	0	1	Europe	Italy
9609	1	1	Europe	Poland
9508	0	1	Europe	Poland
9607	0	1	Europe	Switzerland
8790	1	1	North America	Canada
9505	1	1	North America	Cuba
6613	1	1	North America	USA

8118	1	1	North America	USA
7960	1	1	North America	USA
7498	1	1	North America	USA
6731	0	1	North America	USA
8409	0	1	North America	USA
7003	0	1	North America	USA
7657	0	1	Central America	Mexico
9242	1	1	South America	Ecuador

165

166

TABLE S2 Weather data for outdoor experiment. Radiation data display the cumulative sum of each day. Data were provided from a weather station 5 km distant, and were provided by the Thuringian State Institute for Environment and Geography, Jena, Germany.

		date	Average air temperature [°C]	Global radiation [kWh/m²]	PAR-radiation [kWh/m²]	UV-A [Wh/m²]	UV-B [Wh/m²]
genotype 7498	experiment with	19/07/2017	24	6.8	1.2	263.1	8
		20/07/2017	20.9	4.1	0.8	168.5	5.1
		21/07/2017	22.2	6.1	1.1	239.7	7.2
		22/07/2017	20.8	4.2	0.8	180.4	5.7
		23/07/2017	20	5	0.9	202.7	6.1
		24/07/2017	15.4	1.8	0.4	85.6	2.6
		25/07/2017	14.6	2.2	0.5	102.7	2.9
genotypes for fitness assay	experiment with world-wide distributed	05/09/2016	16.6	2.1	0.4	178.8	3
		06/09/2016	17.9	3.1	0.6	220.7	3.7
		07/09/2016	17.6	5.1	0.9	341.2	5.5
		08/09/2016	20.2	5.2	0.9	339.7	5.5
		09/09/2016	20.9	4.4	0.8	293.2	4.8
		10/09/2016	20.5	4.5	0.8	295.7	4.8
		11/09/2016	21.5	4.1	0.7	275.7	4.5
		12/09/2016	22.6	4.7	0.8	306.4	4.9
		13/09/2016	22.9	4.7	0.8	303	4.8
		14/09/2016	22.2	4.4	0.7	278.3	4.4
		15/09/2016	21.3	4.7	0.8	299.2	4.7
		16/09/2016	18.1	2.2	0.4	158.3	2.5
		17/09/2016	15.5	0.3	0.1	37.9	0.6
		18/09/2016	14.9	1.1	0.2	93.4	1.6
		19/09/2016	13.7	1.7	0.3	136.9	2.2

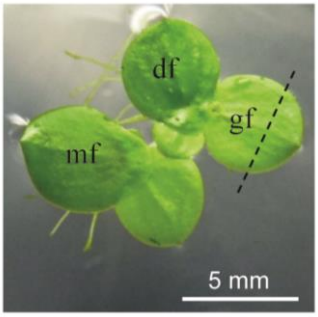

FIGURE S1 *S. polyrhiza* mother fronds (mf), first daughter frond (df) and first granddaughter frond (gf). Line marks axis where gf frond was hand cross-sectioned to stain and visualize flavonoid glucosides.

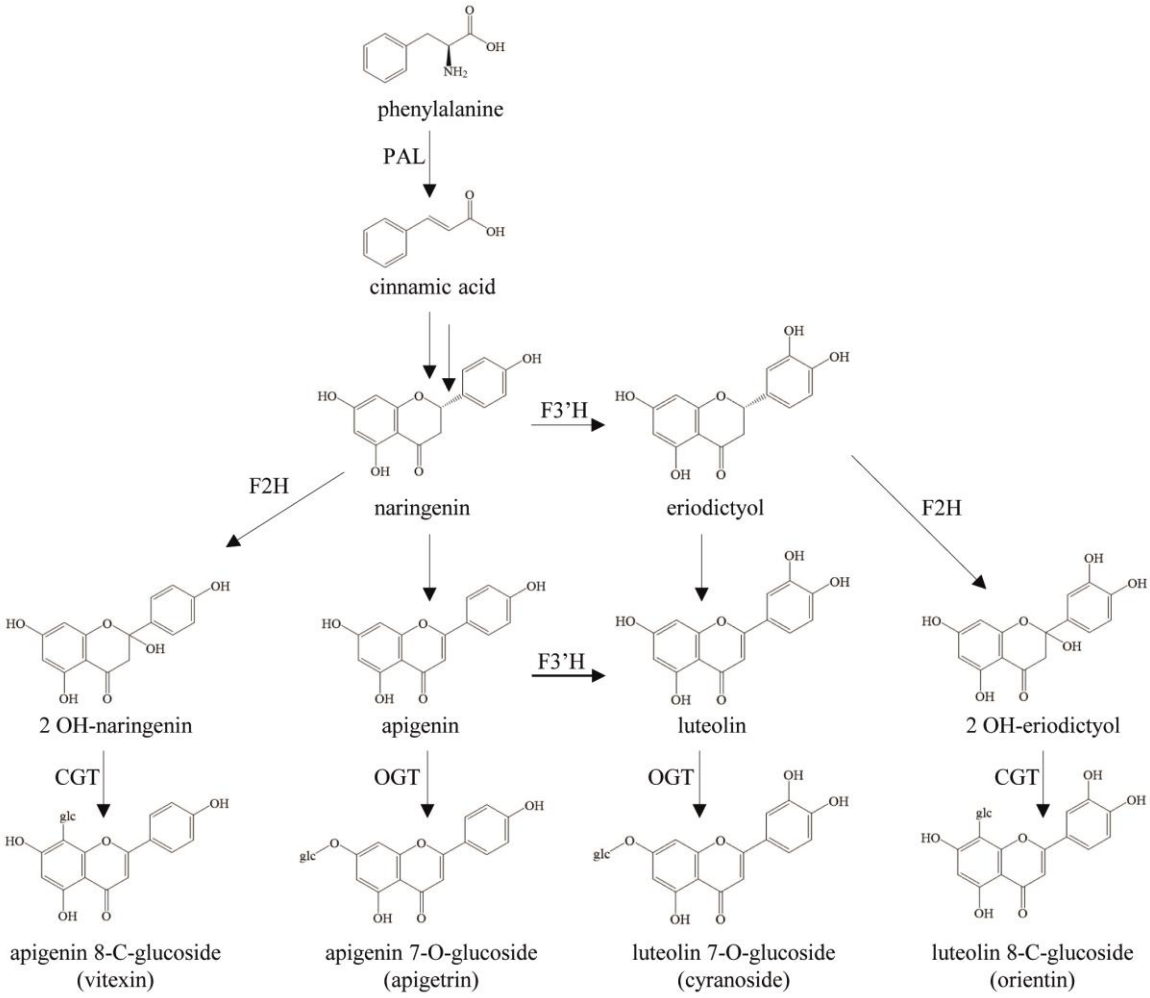

177

178 **FIGURE S2** Scheme of the putative biosynthetic pathway of the major flavonoids in *Spirodela*
179 *polyrhiza* adapted from *Arabidopsis thaliana* and *Zea mays* (Li, Bonawitz, Weng & Chapple 2010;
180 Casas, Duarte, Doseff & Grotewold 2014; Nugroho, Choi & Park 2016). Double arrows represent
181 several steps. Dotted arrow represents less favoured pathway. PAL = phenylalanine ammonia lyase.
182 F2H = flavanone-2-hydrohylas. F3'H = flavonoid 3'-hydroxylase. CGT = C-glycosyl transferase. OGT
183 = O-glycosyl transferase

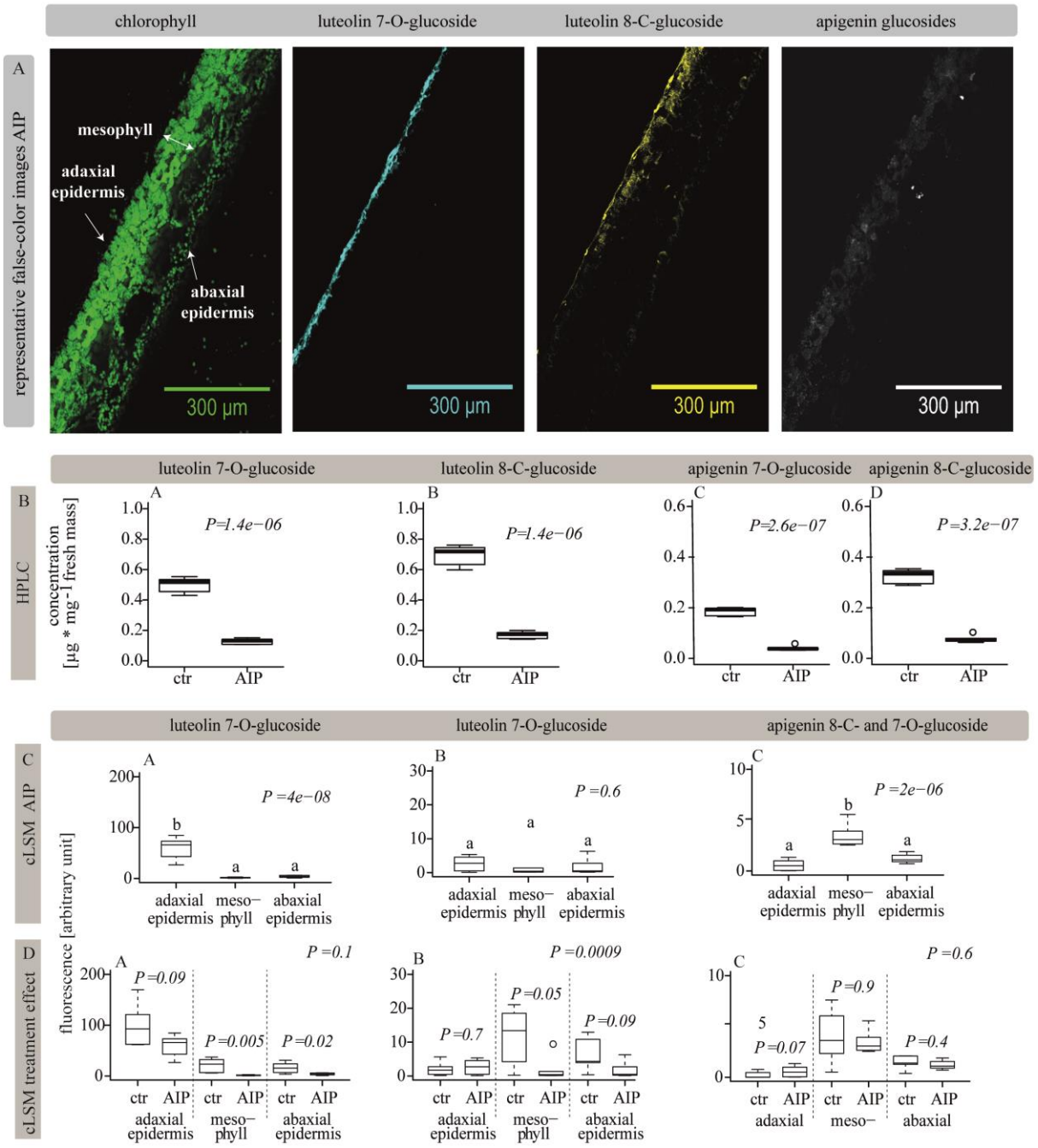

184

185 **FIGURE S3** (A) cLSM false-color-images of 2-APB-stained *Spirodela polyrhiza* cross-sections of
186 plants growing in the presence of the phenylalanine ammonia-lyase (PAL)-inhibitor 2-aminoidane-2-
187 phosphonic acid (AIP). Brightness and contrast were adapted in ImageJ for demonstrative reasons. (B)
188 Whole plant flavonoid glucoside content was reduced after exposure to the PAL-inhibitor AIP. Mean
189 levels of control and AIP exposed plants were analysed with Student's *t*-test. The second generation

(granddaughters) of plants that had been subjected to the individual condition was analysed. (C) Tissue distribution of individual flavonoid glucosides via fluorescence-based quantification was altered by AIP. Statistics of likelihood ratio tests comparing two linear mixed effect models that differ in the factor tissue layer as a fixed effect are shown. Different lower-case letters indicate significant differences in fluorescence intensity according to Tukey's HSD test. (D) Comparison of tissue distribution of individual flavonoid glucosides (fluorescence-based quantification) by AIP treatment and controls. AIP had tissue-specific effects on flavonoid accumulation particularly on luteolin levels. *P*-values of likelihood ratio tests comparing two linear mixed effect models that differed in the interaction term of treatment and tissue layer are displayed above each figure. Wilcoxon-Mann-Whitney-Tests were then used to test for differences of individual flavonoid fluorescence intensities between treatments within a tissue layer. Plants were grown in the absence and presence of AIP until the granddaughter generation had matured (day 6). ctr = control. AIP = 2-aminoidane-2-phosphonic acid. n = 6.

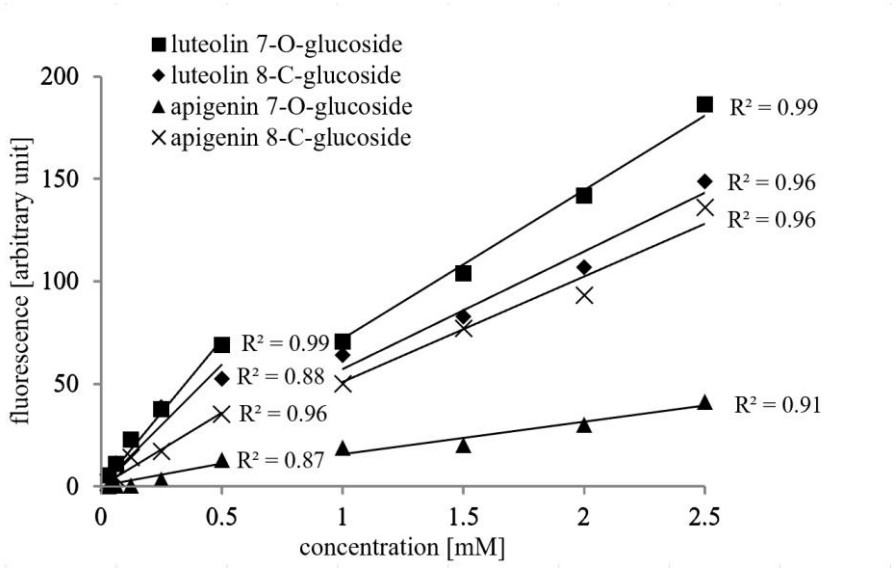

FIGURE S4 Fluorescence intensities of individual synthetic flavonoid glucosides for two concentration ranges when stained with 2-APB (2-aminoethyl diphenylborinate). Concentration levels refer to final flavonoid glucoside concentrations after 1:1 addition of 0.25 % 2-APB solution. Linear regressions of two concentration ranges were applied due to non-linearity of the correlations.

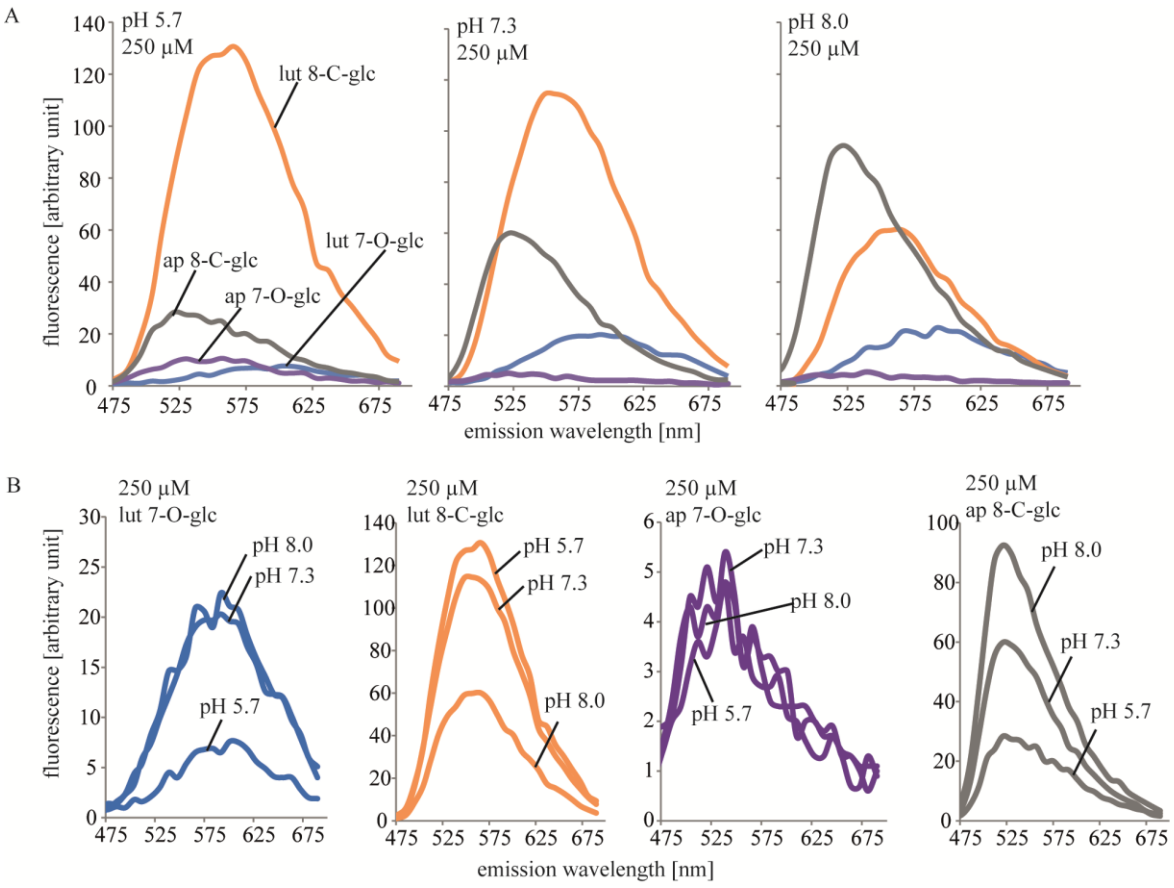

FIGURE S5 Effect on pH on fluorescence emission spectra of individual synthetic flavonoid glucosides. Individual compounds were dissolved in phosphate buffer of pH 5.7, 7.3 and 8.0 and stained with 2-APB (2-aminoethyl diphenylborinate) (1:1) with a final flavonoid glucoside concentration of 250 µM. (A) Comparison of defined pH value among compounds. (B) Comparison of compounds among different pH values. Intensities of apigenin 7-O-glc likely underrepresent true intensities due to formation of crystals at acidic conditions.

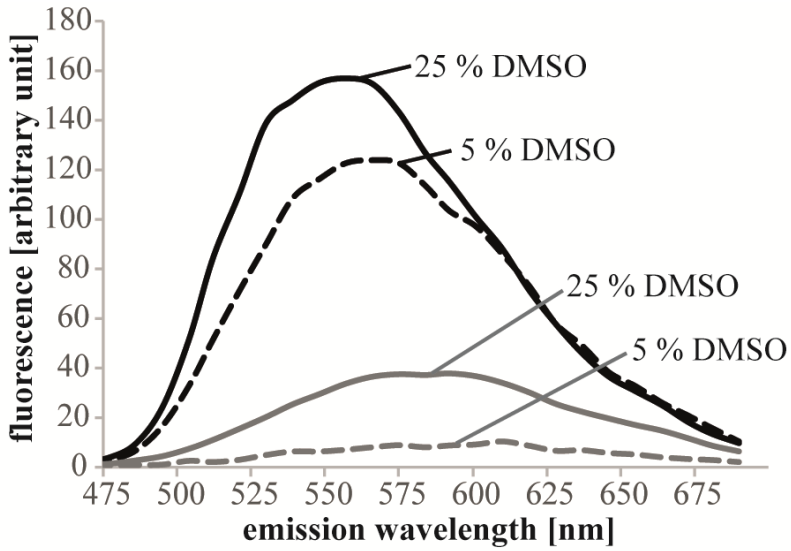

FIGURE S6 Effect of DMSO concentration on fluorescence emission spectra of luteolin glucosides. Luteolin 8-C-glucoside (black) and luteolin 7-O-glucoside (grey) were dissolved in 25% or 5% DMSO concentration in phosphate buffer (pH=7.3) at a final flavonoid concentration of 500 µM.

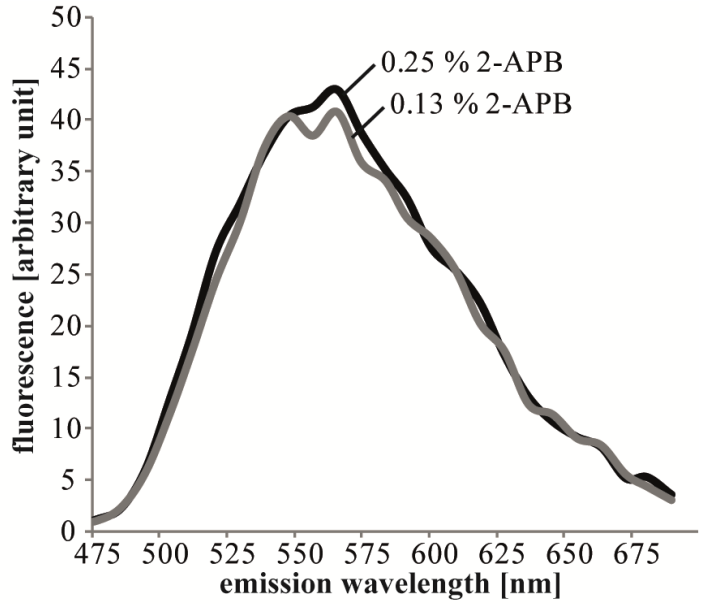

FIGURE S7 Effect of 2-APB (2-aminoethyl diphenylborinate) on fluorescence emission spectra of luteolin 8-C glucoside (100 µM, pH 7.3 in phosphate buffer) when stained 1:1 with either 0.25 % or 0.13 % 2-APB solution.

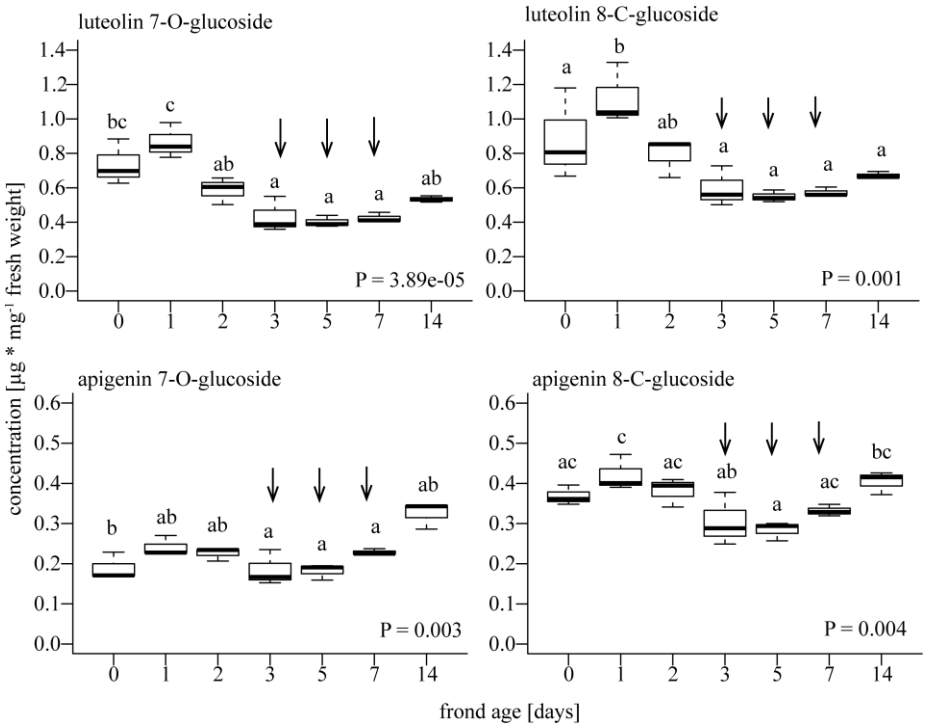

FIGURE S8 Individual flavonoid concentrations of *S. polyrhiza* fronds over frond lifespan. All following experiments were performed with plants between age 3-7 days when flavonoid content was most stable (indicated by arrows). Data were analysed with one-way ANOVAs. Different lower case letters indicate significant differences according to Tukey's post hoc tests. n =3.

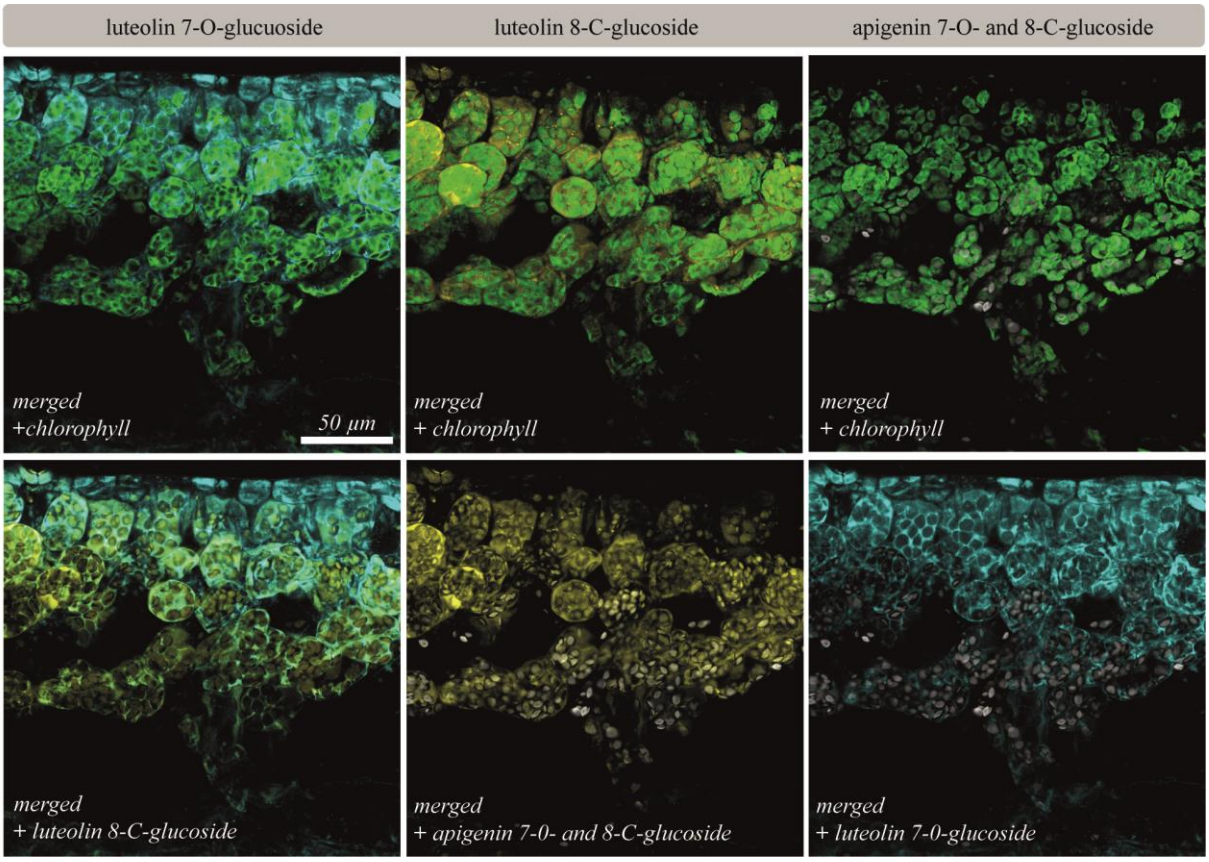

238

239 **FIGURE S9** Corresponding merged channels of images of Figure 3. Subcellular distribution of
240 individual flavonoid glucosides based on cLSM false-colour-images of a 2-APB stained *Spirodela*
241 *polyrhiza* cross-section. Brightness and contrast of all images were adapted in ImageJ for illustrative
242 purpose. 2-APB = 2-aminoethyl diphenylborinate.

243

244

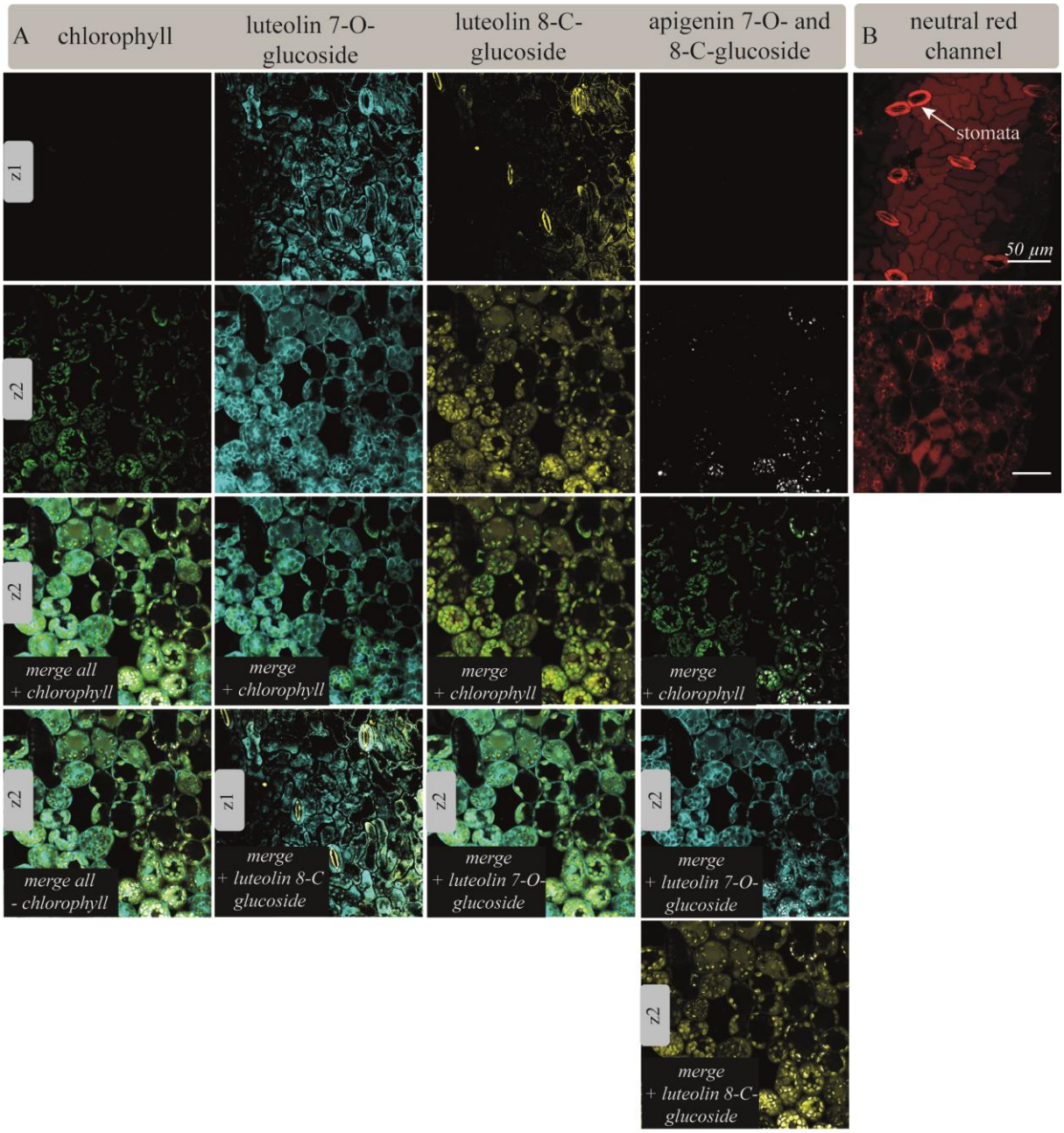

FIGURE S10 cLSM false-colour-images of DBPA and neutral red-stained *Spirodela polyrhiza* fronds. View on the adaxial epidermis at two different depths (z1- top, z2- deeper) to show the subcellular distribution of individual flavonoid glucosides. Both luteolin glucoside channels showed fluorescence comparable with the neutral red (vacuolar) channel. Luteolin 8-C-glucoside additionally showed overlay with the chlorophyll (chloroplast) channel. Apigenins mostly accumulated in deeper cell layers. cLSM was performed with the 'online fingerprinting' feature. 2-APB-stained cross-sections were excited at 405 nm; in another cross-section neutral red-stained sections were excited at 543 nm. Brightness and

contrast of all images were adapted individually in ImageJ for demonstrative reasons. 2-APB = 2-aminoethyl diphenylborinate. Scalebars correspond to 50 µm.

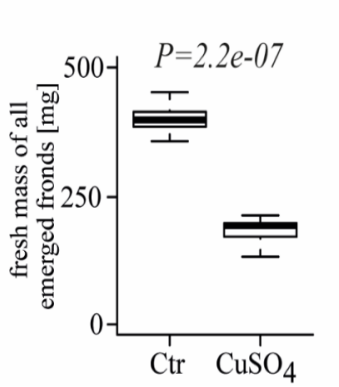

FIGURE S11 Reduction of fresh weight of fronds grown in the presence of copper sulphate (*S. polyrhiza* genotype 7498). Mean weights of control and copper sulphate exposed plants were analysed with Student's *t*-test. n = 6. ctr = control

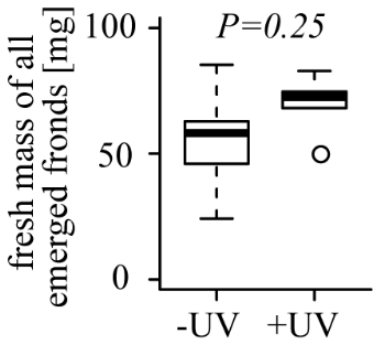

FIGURE S12 Fresh weight of fronds was not affected by UV treatment (*S. polyrhiza* genotype 7498). Mean weights of control and UV exposed plants were analysed with Student's *t*-test. n = 5.

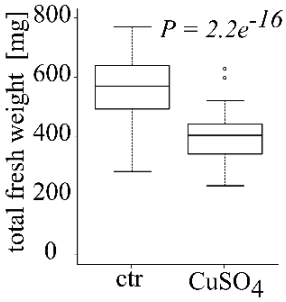

FIGURE S13 Reduction of fresh weight of fronds grown in the presence of copper sulphate in 53 *S. polyrhiza* genotypes. Mean weights of control and copper exposed plants (n=3) were analysed with Student's *t*-test. ctr = control

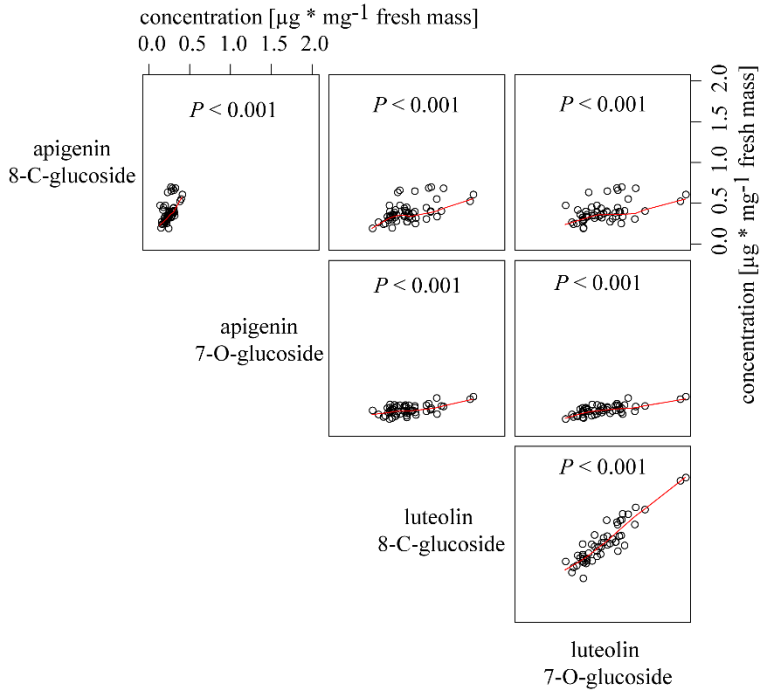

FIGURE S14 Concentrations of individual flavonoid glucosides were highly correlated across 53 *S. polyrhiza* genotypes exposed to copper sulphate. *P*-values of Pearson's correlation coefficients are shown. Each data point indicates the mean flavonoid concentration of one clone growing under control conditions.

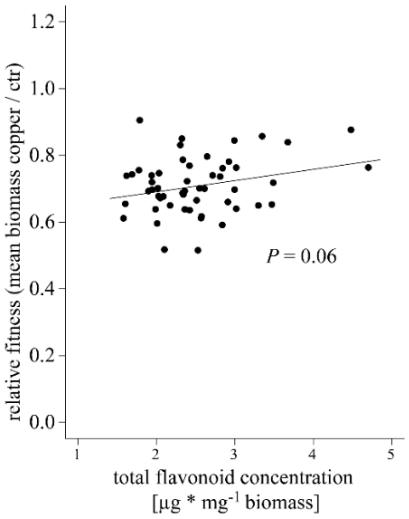

277

278 **FIGURE S15** Total flavonoid concentration was weakly correlated to relative plant fitness across 53 *S.*

279 *polyrhiza* genotypes under copper sulphate treatment. *P*-value of linear model is shown. ctr = control

280

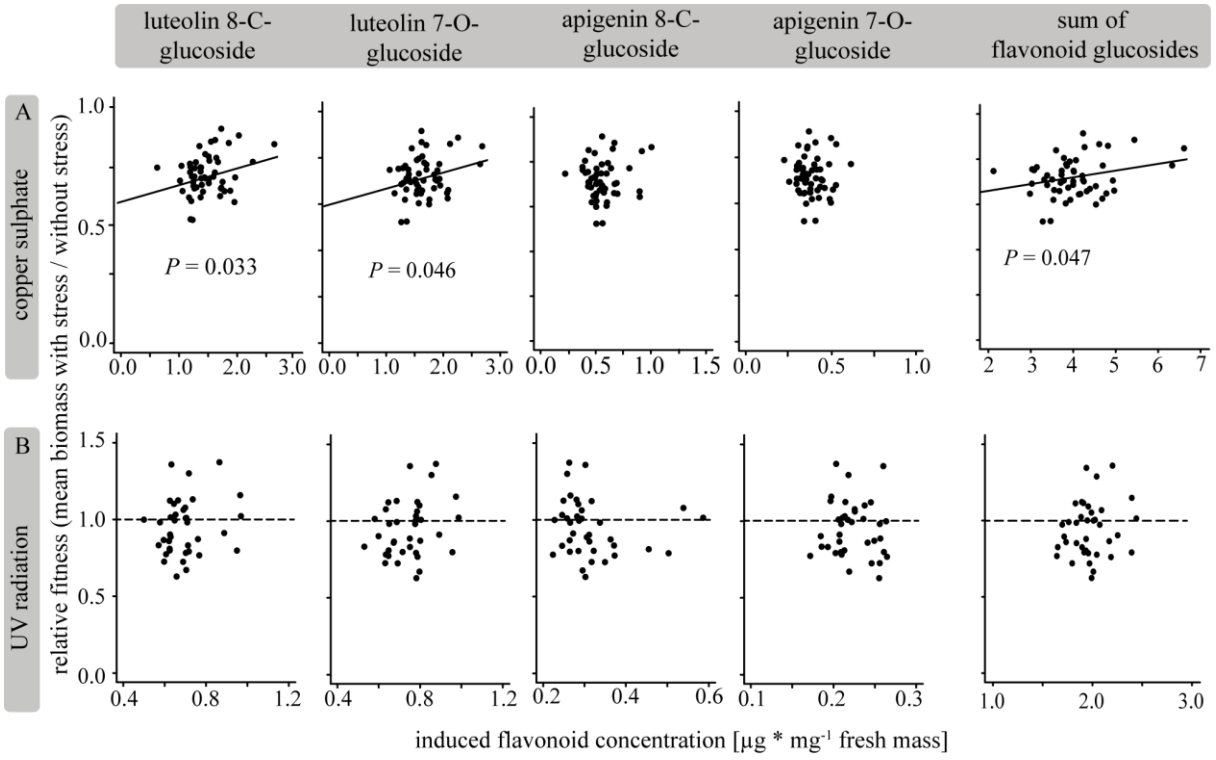

281

282 **FIGURE S16** Correlation of relative fitness (mean biomass accumulation with stress / without stress)

283 and induced flavonoid concentration across of 53 *S. polyrhiza* genotypes under (A) copper sulphate and

(B) UV treatment. Each data point represents the mean of one genotype. *P*-values of linear models based on mean values per genotype are shown.

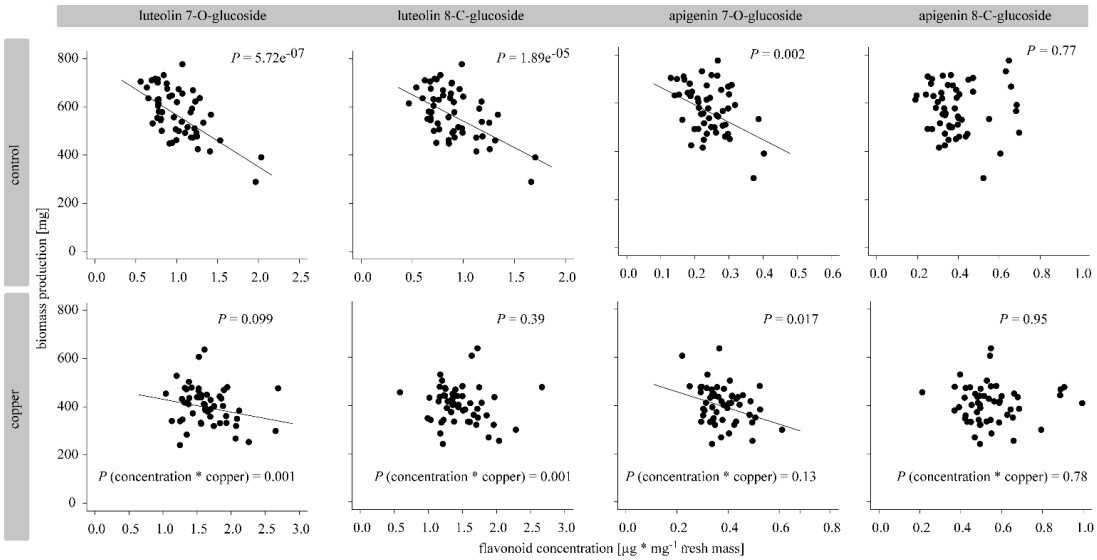

FIGURE S17 Correlation of biomass production and individual flavonoid concentration across of 53 *S. polyrhiza* genotypes under control and copper sulphate treatment. The correlations between biomass production and individual as well as total flavonoid concentration in the presence and absence of $CuSO_4$ were analysed using linear models based on the mean value of each treatment and genotype.

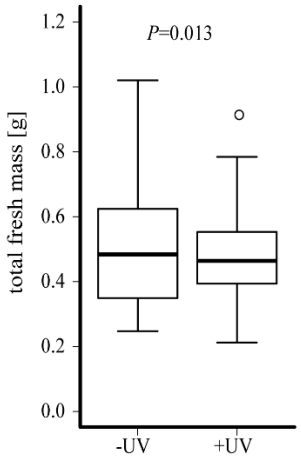

295

296 **FIGURE S18** Total fresh mass of fronds across 38 *S. polyrhiza* genotypes was reduced by an aerage of
297 8% in the presene of natural UV radiation. Mean weight of UV shielded (-UV) and UV exposed (+UV)
298 plants were analysed with Student's *t*-test.

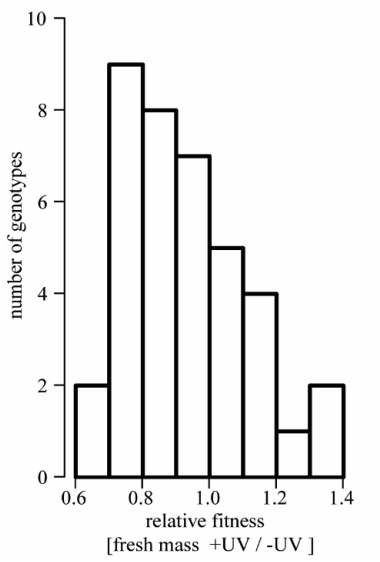

299

300 **FIGURE S19** Distribution of 38 *S. polyrhiza* genotypes depending on the relative fitness under UV
301 exposure. The majority of genotypes showed reduced fitness but 30% showed increased fitness.

302

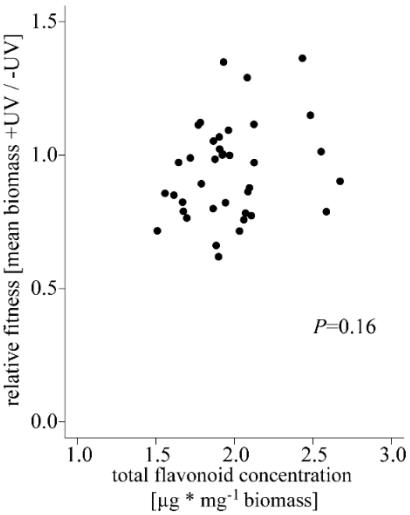

FIGURE S20 Total flavonoid concentration did not correlate to relative plant fitness across 38 *S. polyrhiza* genotypes under natural UV light exposure. *P*-value of linear model is shown.

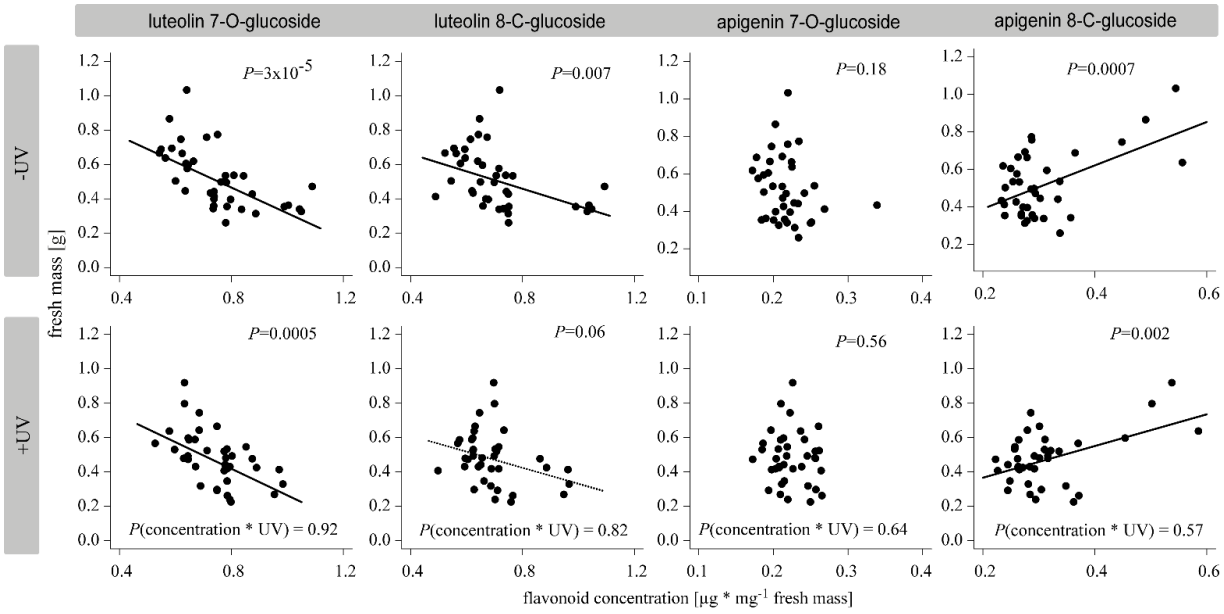

FIGURE S21 Correlation of biomass production and individual flavonoid concentration across 38 *S. polyrhiza* genotypes in the presence and absence of natural UV light. The correlations between biomass production and individual as well as total flavonoid concentration in the presence and absence of UV light were analysed using linear models based on the mean value of each treatment and genotype.

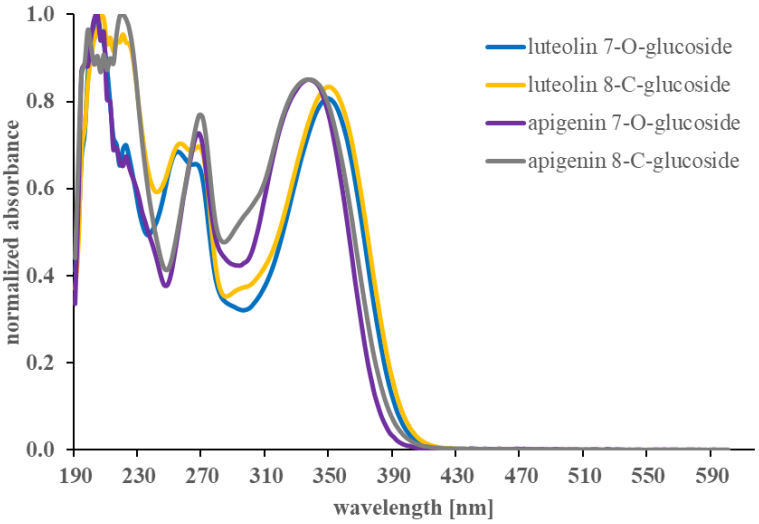

313

314 **Figure S22** UV spectra of flavonoid glucosides. Absorbance was normalized for each compound

315 separately.

316 **REFERENCES**

317 Appenroth K.-J. & Crawford D.J. (2015) After the genome sequencing of duckweed – how to proceed
318 with research on the fastest growing angiosperm? *Plant Biology*, 17, 1–4.

319 Appenroth K.J., Borisjuk N. & Lam E. (2013) Telling duckweed apart: Genotyping technologies for
320 the Lemnaceae. *Chinese Journal of Applied and Environmental Biology*, 19, 1–10.

321 Cabrera L.I., Salazar G.A., Chase M.W., Mayo S.J., Bogner J. & Dávila P. (2008) Phylogenetic
322 relationships of aroids and duckweeds (Araceae) inferred from coding and noncoding plastid
323 DNA. *American Journal of Botany*, 95, 1153–1165.

324 Casas M.I., Duarte S., Doseff A.I. & Grotewold E. (2014) Flavone-rich maize: An opportunity to
325 improve the nutritional value of an important commodity crop. *Frontiers in Plant Science*, 5, 1–
326 11.

327 Cusimano N., Bogner J., Mayo S.J., Boyce P.C., Wong S.Y., Hesse M., … French J.C. (2011)
328 Relationships within the Araceae: Comparison of morphological patterns with molecular
329 phylogenies. *American Journal of Botany*, 98, 654–668.

330 Harrell Jr F.E. & Dupont C. (2015) Hmisc: Harrell Miscellaneous. *R package*,.

331 Hegelmaier F. (1895) Systematische Übersicht der Lemnaceen. *Botanische Jahrbücher der*
332 *Systematik, Pflanzengeschichte, und Pflanzengeographie*, 21, 268–305.

333 Li X., Bonawitz N.D., Weng J.K. & Chapple C. (2010) The growth reduction associated with
334 repressed lignin biosynthesis in Arabidopsis thaliana is independent of flavonoids. *Plant Cell*, 22,
335 1620–1632.

336 Nauheimer L., Metzler D. & Renner S.S. (2012) Global history of the ancient monocot family Araceae
337 inferred with models. *New Phytologist*, 195, 938–950.

338 Nugroho A., Choi J.S. & Park H.J. (2016) Analysis of flavonoid composition of Korean herbs in the
339 family of compositae and their utilization for health. *Natural Product Sciences*, 22, 1–12.

340 Sree K.S., Bog M. & Appenroth K.J. (2016) Taxonomy of duckweeds (Lemnaceae), potential new
341 crop plants. *Emirates Journal of Food and Agriculture*, 28, 291–302.

342